**Rare Metal Materials and Engineering**
Volume 49, Issue 6, June 2020
Available online at www.rmme.ac.cn

Science Press

**Cite this article as:** Rare Metal Materials and Engineering, 2020, 49(6): 1907-1914.

ARTICLE

# Wettability and Spreading Dynamics Analysis of Al-Mg Alloys on 2D-Gr Fabrics

**Wang Chenchong[1], Huang Minghao[1], Zhang Qiuhong[1], Wang Xu[2]**

*[1] State Key Laboratory of Rolling and Automation, Northeastern University, Shenyang 110819, China; [2] Liaoning Shihua University, Fushun 113001, China*

**Abstract:** The wetting behavior of Al-Mg alloys with different Mg amounts (3.2 wt%, 4.5 wt%, 6.5 wt%, 8.5 wt%, 10 wt%, 13 wt%, 17 wt%) on M40 graphite fabrics was investigated by sessile drop method. The effect of Mg amount on the wettability and spreading behavior was discussed. The initial contact angle decreases from 115º in Al-3.2Mg/graphite fabrics to 88.5º in Al-17Mg/graphite fabrics system. The final contact angle decreases from 96.7º in Al-3.2Mg/graphite fabrics to 71º in Al-17Mg/graphite fabrics system. The initial contact angle measured on porous M40 graphite fabrics is lower than reported results on dense carbon plates due to the surface microstructure of M40 fabrics. Since surface tension of Al-Mg alloys decreases, the initial and final contact angles decrease with increasing of Mg amount. According to Dezellus equation, the kinetic constant ($k$) in spreading behavior was obtained from data fitting of experimental results. Miedema model was introduced in the present work to calculate the theoretical $k$. The experimental or theoretical $k$ changes little with increasing of Mg amount. Moreover, theoretical calculation values of $k$ are very close to the experimental results, which indicates the applicability of Miedema model to the calculation of kinetic constant.

**Key words:** composite; wetting; spreading; Al-Mg alloys; graphite fabrics

Carbon fiber reinforced aluminum matrix composites have been receiving considerable application in aerospace industry because of their low density[1], high specific modulus and strength[2], and excellent thermal properties[3]. Moreover, graphite fabrics, which demonstrate low reaction activity with aluminum matrix, are more suitable to use as reinforcement ($Gr_f$/Al)[4]. However, it is difficult to prepare dense $C_f$/Al composites due to poor wettability between graphite and the molten Al alloys[5]. The infiltration process of molten Al alloys into graphite fabric bundles is strongly related to their wettability. Therefore, in order to optimize the preparation process, it is indispensable to understand and improve the wettability between carbon fabrics and molten Al alloys.

Landry et al. [6] investigated the wetting behavior between carbon substrates (vitreous carbon, pyrolytic carbon and graphite pseudo single crystals) and Al alloys (pure Al, Al-Si, and Al-Ti) by sessile drop technique under high vacuum. It was reported that Al alloys tested in their work did not wet carbon regardless of graphite material below 1273 K[6]. These results are consistent with investigation of Nakae et al[7]. Numerous research studies have been carried out to overcome the wetting drawback. Imposing extra energy (pressure or ultrasonic) to force molten Al infiltrated into interfibre space is the effective method. Gas pressure infiltration[8-10], ultrasonic infiltration[5,11,12] and squeeze casting[13-15], have been adopted to fabricate dense $C_f$/Al composites. Coating an intermediate layer on carbon fabrics' surface has been also reported to be beneficial to infiltration process. Ni[16-18] and Cu[17-19], which could be well wetted by Al alloys, have been evaluated. Addition of alloying elements into Al alloys is the simplest way to modify the carbon-Al wettability. Si[6,7,20] and Mg[11,20-22] could decrease surface tension of Al alloys and improve the carbon-Al wettability. Moreover, addition of Mg could inhabit the formation of $Al_4C_3$ significantly[23], leading

Received date: June 18, 2019
Foundation item: National Natural Science Foundation of China (51790481); Basic Scientific Research Funds of Northeastern University (N170703004); China Postdoctoral Science Foundation (2018M641698)
Corresponding author: Wang Chenchong, Ph. D., Lecturer, State Key Laboratory of Rolling and Automation (RAL), Northeastern University, Shenyang 110819, P. R. China, Tel: 0086-24-83680246, E-mail: wangchenchong@ral.neu.edu.cn

Copyright © 2020, Northwest Institute for Nonferrous Metal Research. Published by Science Press. All rights reserved.

to improvement in mechanical properties[24]. However, the effect of Mg on the wettability and spreading dynamics of C-Al system is rarely reported.

In the present work, the effect of Mg amount on the wettability and spreading dynamics of Al alloys on the two dimensional (2D) graphite fabrics were investigated. Dezellus and Miedema model were adopted to analyze their wetting behavior.

## 1 Experiment

Al-Mg alloys with Mg content of 3.2 wt%, 4.5 wt%, 6.5 wt%, 8.5 wt%, 10 wt%, 13 wt% and 17 wt% were prepared from 99.99 wt% Al and 99.95 wt% Mg (Supplied by Northeast Light Alloy Co., Ltd). Before experiment, samples of Al-Mg alloys were cut to $\Phi$3.5 mm×3 mm cylinder, washed by 5% NaOH solution and 5% HF solution at room temperature for 3 min and then stored in alcohol solution. Since the surface microstructure of substrates has great effect on the wetting behavior [25], 2D graphite fabrics with dimension of 20 mm×20 mm×5 mm instead of high pure graphite plates were used in the present work in order to simulate the actual situation. The typical microstructure of the fabrics is shown in Fig.1. During weaving process, the graphite fabric bundles cross over and under each other and are crimped or bent on a short radius, which is different to the smooth surface of normal graphite or ceramic substrates.

The wetting behavior was investigated by sessile drop method. Wetting experiments were carried out on CXZ-20 high temperature interfacial property instrument in Beihang University. The system was composed of a sealed chamber, a bottle of Ar gas, a set of vacuum pumps, dropping tube and a CCD video camera. The chamber was evacuated to $2\times10^{-3}$ Pa at room temperature, and then high pure Ar was introduced into the chamber up to $1.0\times10^{5}$ Pa to prevent oxidation during test. In order to limit evaporation of aluminum and its alloys at high temperature, the chamber was re-evacuated to $2\times10^{-3}$ Pa at room temperature at the beginning of the experiment, and the samples were then heated at 10 K/min to 1273 K under $2\times10^{-3}$ Pa in a dynamic vacuum of controlled Ar micro-leaks. The carbon fabric was moved to the bottom of dropping tube before re-evacuation. Afterward, molten aluminum alloy was dropped by pressure difference between chamber and dropping tube. The droplet was observed with a CCD video camera for 900 s after dropping. Contact angles and drop base radii were measured directly from the image of the drop section with an accuracy of ±2° and 2%, respectively. All tests have been performed on at least three samples, in order to improve statistical significance of the results. The testing methods for all the samples with different Mg contents were the same.

Philips CM-12 TEM equipment with the voltage of 120 kV was used to observe the microstructure of C/Al system. XRD was used to identify the phase in C/Al system. HRTEM and EDS was used to explain the structure and composition of the reactant. XRD analysis was carried out by Rigaku D/max-rB diffractometer. The specimens were subjected to Cu-Kα radiation with a scanning speed set at 2°/min.

## 2 Results and Discussion

### 2.1 Contact angles

Wetting is usually characterized by the contact angle ($\theta$), which relates with the interfacial energies of the solid/liquid/vapor system. If the contact angle is greater than 90°, the graphite fabrics are not wetted by the molten Al, and then external force is necessary to infiltrate molten Al into bundle of fabrics during preparation. The contact angle could be calculated by Young's equation (Eq.1)[26] and classic Young-Dupré equation (Eq.2)[6]:

$$\cos\theta = \frac{(\sigma_{sv} - \sigma_{sl})}{\sigma_{lv}} \quad (1)$$

$$W_A = \sigma_{lv}(1+\cos\theta) \quad (2)$$

where $\sigma_{sv}$, $\sigma_{sl}$ and $\sigma_{lv}$ are solid/vapor, solid/liquid and liquid/vapor interfacial energies, respectively. $W_A$ represents the work of adhesion between the liquid and the substrate.

Variation of contact angles of Al-Mg alloys on graphite fabrics with time at 1273 K is shown in Fig.2[27]. All curves consist of three kinetic stages, and the wetting kinetics could

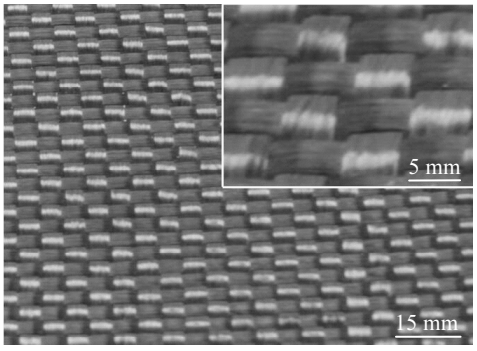


Fig.1 Morphology of 2D-Gr reinforcement

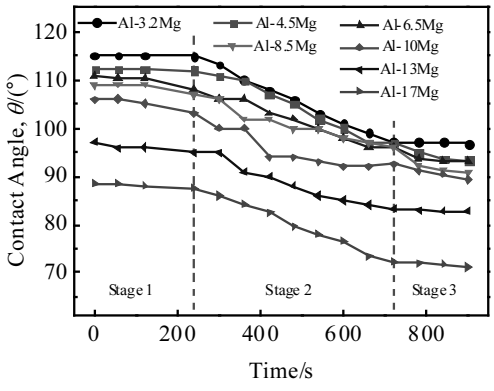


Fig.2 Variation of instantaneous contact angle with time

be characterized by the values of contact angles. In the first stage (<240 s), the relationships between the contact angles and time are flat line. In the second stage (240~720 s), contact angles decrease are observed in all Al-Mg alloys. In the third stage (720~900 s), the contact angles remain steady, and change slightly with time. In order to illustrate the effect of Mg, variation of initial and final contact angles with Mg amount is shown in Fig.3. It is obvious that the initial and final contact angles decrease with increase of Mg amount. The initial contact angle decreases from 115º in Al-3.2Mg/graphite fabrics to 88.5º in Al-17Mg/graphite fabrics system. The final contact angle decreases from 96.7º in Al-3.2Mg/graphite fabrics to 71º in Al-17Mg/graphite fabrics system.

There are a great number of researches on the wetting behavior of Al/C system. However, the experimental data below 1273 K are very scattered and even conflicting with each other. The final contact angle reported varies from about 30º to 160º [6,22,28,29] at 1273 K. Moreover, Landry et al[6,28,29] reported the contact angles of Al/C decreased rapidly from 160º to 135º within initial 400 s and then reached the platform. However, no significant effect of holding time on contact angles in Al/C system was observed by Yoshida et al[22]. These variations could be attributed to several factors: (i) the aluminum oxide layer on the surface of molten Al; (ii) the reaction between molten Al and graphite substrates; (iii) the amount of alloying elements; (iv) the porosity, roughness and microstructure of graphite substrates. Landry et al[29] reported that the contact angle of Al/C system without reactions is 139º, and similar values have also been reported in other literature for the wettability testing on dense carbon plates[22,28]. However, in the present work, the initial contact angle in Al-3.2Mg/graphite fabrics is 115º, which is in the condition without reactions, much lower than their results on dense carbon plates.

For several previous researches in Al-Mg alloys with relatively high Mg content, no reaction was supposed to take place at the initial stage during testing[30,31]. However, composition of Al-3.2Mg alloys in the present work is similar to that of the alloys used by Yoshida et al, which considered interface reaction as an important factor[22]. Therefore, reaction and effect of Mg addition should be considered for further explanation, and they are also the main factors discussed in Part 2.2. Furthermore, porosity of substrate would decrease the measured contact angle if the actual contact angle (measured on an ideal flat substrate with no roughness) is less than 90º; otherwise, porosity of substrate would result in the increase of measured contact angle when the actual contact angle is greater than 90º [32-35]. In the present work, the measured contact angles in Al-3.2Mg/graphite fabrics (115º) are greater than 90º, indicating the porosity of graphite fabrics should not be responsible for the large decrease in contact angles. Thus, the microstructure of graphite fabrics should also be considered as one of the reasons for the decrease of contact angle. Actually, Yoshida et al[22] tested the contact angle between molten Al and basal plane, prismatic plane or isotopic graphite at 1189 K. The initial contact angles for basal plane, prismatic plane and isotopic graphite were about 125º, 148º and 166º, respectively. Moreover, due to graphitization process, microstructures of graphite fiber surface are mainly composed of graphitic basal planes and prismatic edge surfaces, while the latter structures are considered to be highly reactive[36,37]. Therefore, the measured initial contact angles in Al-3.2Mg/graphite fabrics (115º) is reasonable, considering higher temperature tested in the present work.

Furthermore, it is reported that the surface tension of Al-Mg alloys decreased with increasing of Mg amount[38]. This phenomenon was also observed by Yoshida et al[22] that the surface tension of Al-Mg alloys decreased from 0.99 N/m of pure Al to 0.73 N/m of Al-9.1Mg. Therefore, the initial and final contact angles tested in the present work decrease with increasing of Mg amount.

### 2.2 Spreading rates

Fig.4 shows the XRD pattern of Al/C system which proves the existence of $Al_4C_3$. Fig.5 shows the morphologies of $Al_4C_3$ in C/Al-0Mg system observed by TEM. Fig.6 shows the TEM morphology of $Al_4C_3$ in C/Al-4.5Mg system. According to Fig.5 and Fig.6, there is visible reactant $Al_4C_3$ at the interface of both C/Al and C/Al-Mg system. A single $Al_4C_3$ is needle-like; however, a large amount of $Al_4C_3$ can form an obvious

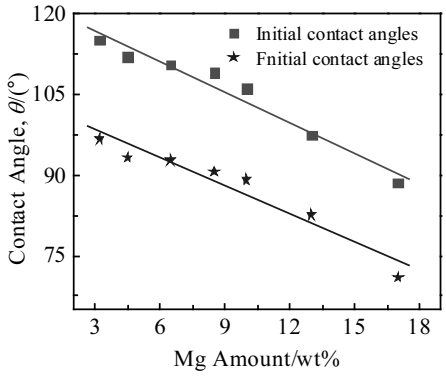


Fig.3 Variation of initial and final contact angles with Mg amount

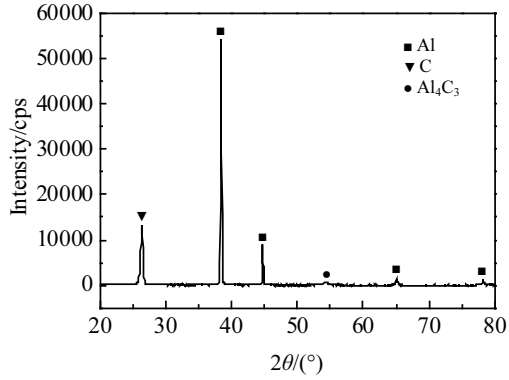


Fig.4 XRD pattern of C/Al system

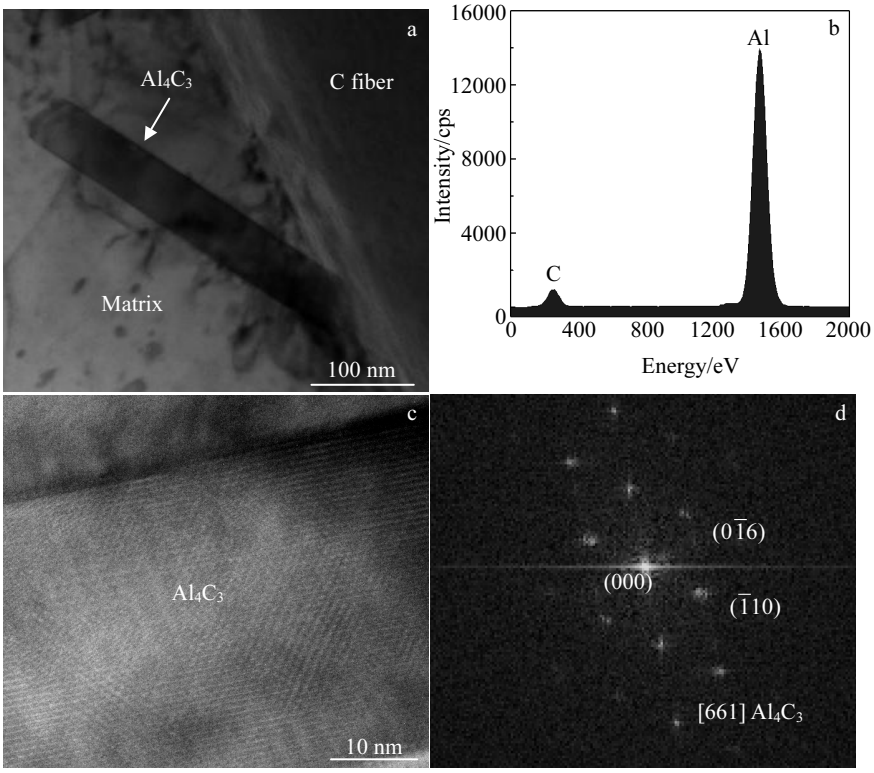


Fig.5 TEM image (a), EDS spectrum (b), HRTEM image (c), and SAED pattern (d) of $Al_4C_3$ in C/Al-0Mg system

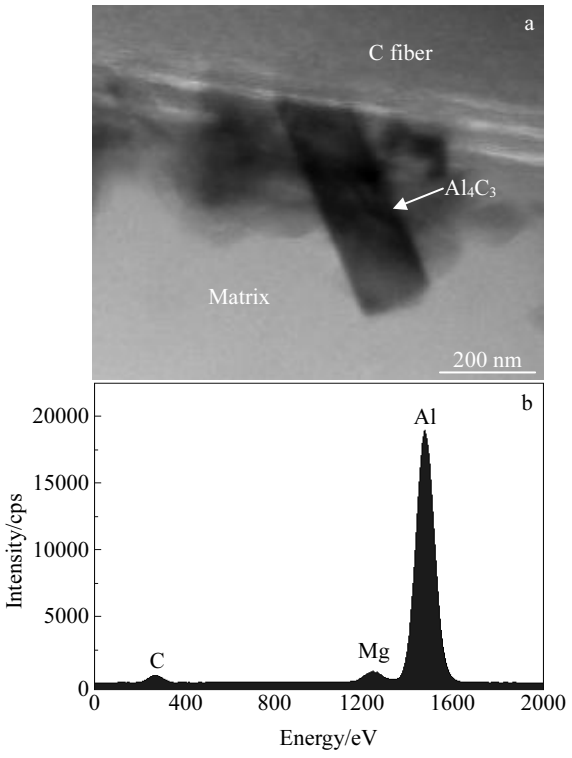


Fig.6 TEM morphology (a) and EDS spectrum (b) of $Al_4C_3$ in C/Al-4.5Mg system

reactant layer at the interface, as shown in Fig.7. This kind of $Al_4C_3$ layer which was also observed by Landry et al[6] can affect the wettability and spreading dynamics significantly. Although addition of Mg element could decrease the growth and nucleation of $Al_4C_3$ phase[23,24], the reaction between Al and graphite fabrics is inevitable during high temperature wetting process (1273 K)[4,13,39]. After the formation of $Al_4C_3$ phase near triple line, the wetting behavior changes from Al/C to Al/$Al_4C_3$+C (discontinuous $Al_4C_3$) or Al/$Al_4C_3$ system (continuous $Al_4C_3$). Since the $Al_4C_3$ phase could be better wetted by molten Al than initial graphite surface, the contact angles decrease with time (stage 2 in Fig.2). This behavior is called as

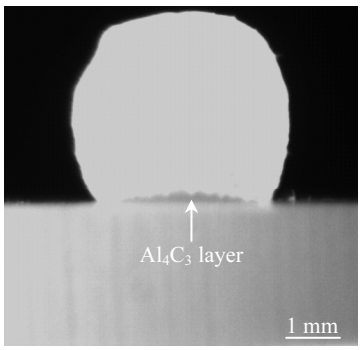


Fig.7 Reactant layer at the interface of C/Al-Mg system

decreasing rate spreading (DRS) stage[40,41], and the spreading rates in this stage could be calculated by Dezellus model[40,42].

Generally, equilibrium contact angle ($\theta_E$) could be calculated by Cassie equation:

$$\cos\theta_E = \alpha\cos\theta_P + (1-\alpha)\cos\theta_S \quad (3)$$

where $\theta_P$ and $\theta_S$ are the equilibrium contact angles of liquid phase on reaction product and substrate, respectively.

The coverage rate ($\alpha$) is defined as follows:

$$\alpha = 1 - \frac{S_C}{S_T} \quad (4)$$

where $S_C$ and $S_T$ are surface area not covered by the reaction product and total surface area, respectively.

Since the instantaneous contact angle ($\theta$) is slightly higher than the equilibrium contact angle, Dezellus et al [40] supposed the equation to describe wetting behavior during the DRS stage:

$$\cos\theta = \alpha\cos\theta_F + (1-\alpha)\cos\theta_0 \quad (5)$$

where $\theta_0$ and $\theta_F$ are initial and final contact angles, respectively. Eq.(5) can also be expressed as Eq.(6):

$$\frac{d\theta}{dt} = -\frac{\cos\theta_F - \cos\theta_0}{\sin\theta}\cdot\frac{d\alpha}{dt} \quad (6)$$

Moreover, based on the experiment results, it is concluded that the spreading kinetic is not limited by the diffusion liquid phase or the growth process at the interfaces, but by the process at the dissolution interface in case of Al/C system[40]. Therefore, the reduction rate of the Al/C interface is proportional to the area not covered by the reaction product (Eq.(7)). Furthermore, assuming the total surface area ($S_T$) remains constant during spreading, the above equation could be transformed to Eq.(8):

$$\frac{dS_C}{dt} = -kS_C \quad (7)$$

$$\frac{d\alpha}{dt} = k(1-\alpha) \quad (8)$$

where $k$ is a kinetic constant ($s^{-1}$).

Combining the Eqs.(5), (6) and (8), following expression of $\frac{d\theta}{dt}$ can be derived:

$$\frac{d\theta}{dt} = -\frac{k}{\sin\theta}(\cos\theta_F - \cos\theta) \quad (9)$$

After integration of Eq.(9), Eq.(10) can be obtained:

$$\cos\theta_F - \cos\theta = (\cos\theta_F - \cos\theta_0)\exp(-kt) \quad (10)$$

The spreading rate ($U$) is defined as follows:

$$U = \frac{dR_L}{dt} \quad (11)$$

where $R_L$ is the diameter of droplet on the substrate.

Since the thickness of the reaction product ($Al_4C_3$) is much lower than the droplet size[4,6,24], the volume of the droplet ($V$) could be as constant, and it could be calculated by spherical cap volume equation:

$$V = \pi[\frac{R_L}{\sin\theta} - \frac{R_L}{\sin\theta}(1-\cos\theta)][\frac{R_L}{\sin\theta}(1-\cos\theta)]^2 \quad (12)$$

Combining Eqs.(9), (11) and (12), following expression of $U$ could be obtained[40]:

$$U = k(\frac{3V}{\pi})^{\frac{1}{3}}F(\theta)(\cos\theta_F - \cos\theta) \quad (13)$$

$$F(\theta) = \frac{\sin^4\theta - \cos\theta(2 - 3\cos\theta + \cos^3\theta)}{\sin\theta(2 - 3\cos\theta + \cos^3\theta)^{\frac{4}{3}}} \quad (14)$$

It is obvious that the spreading rate ($U$) is affected by the kinetic constant ($k$) and instantaneous contact angle ($\theta$). Actually, according to Eq.(10), the relationship between $\ln\frac{\cos\theta_F - \cos\theta_0}{\cos\theta_F - \cos\theta}$ and time ($t$) would be linear with the slope equal to $k$. Therefore, $k$ could be calculated from the experimental data. The linear fitting of $\ln\frac{\cos\theta_F - \cos\theta_0}{\cos\theta_F - \cos\theta}$ versus time ($t$) curves is shown in Fig.8.

Dezellus et al[40] proposed that the value of $k$ could also be calculated theoretically:

$$k = k_d \cdot \frac{V^m_{Al_4C_3}}{fe}\Delta\mu \quad (15)$$

Where $k_d$ is the kinetic constant of the dissolution process (considered as $4\times10^{-10}$ $mol\cdot m^{-2}\cdot s^{-1}$ [40]), $V^m_{Al_4C_3}$ is the molar volume of $Al_4C_3$ (considered as 49.56 $cm^3$ [43]), $e$ is the average thickness of the $Al_4C_3$ layer at the interface (considered as about 150 nm[23,44]), and $f$ is a geometrical factor (considered as 1[40]). $\Delta\mu$ represents the driving force of the dissolution process, and could be calculated by Eq.(16)[40]:

$$\Delta\mu \approx RT\ln(\frac{a_{Al}}{a^I_{Al}}) \quad (16)$$

where $R$ is gas constant (8.314 J/mol·K), $T$ is the temperature, $a_{Al}$ and $a^I_{Al}$ represent activity of Al in binary Al-Mg alloy and in formation of $Al_4C_3$.

Moreover, $a^I_{Al}$ and $a_{Al}$ could be obtained from Eq.(17)[40] and Eq.(18), respectively:

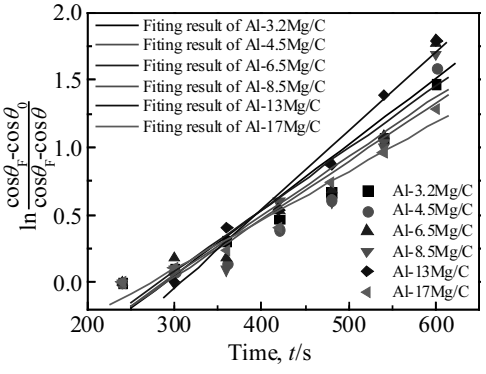


Fig.8 Basic linear regression of $\ln\frac{\cos\theta_F - \cos\theta_0}{\cos\theta_F - \cos\theta}$ versus $t$

$$a_{\mathrm{Al}}^{\mathrm{I}}=\exp\left(\frac{\Delta G_{\mathrm{f}}^{0}(T)}{4RT}\right) \tag{17}$$

$$\alpha_{\mathrm{Al}}=\gamma_{\mathrm{Al}}x_{\mathrm{Al}} \tag{18}$$

where $\gamma_{\mathrm{Al}}$ and $x_{\mathrm{Al}}$ represent the activity coefficient and atom fraction of Al in Al-Mg alloys. $\Delta G_{\mathrm{f}}^{0}(T)$ has been calculated by Lu et al[44] as Eq.(19) in which $T$ is temperature (K):

$$\Delta G_{\mathrm{f}}^{0}(T)=-266266+96.14T \tag{19}$$

The simple method introduced by Wilson to calculate in $\gamma_i$ multiple components is as Eq.(20)[45]:

$$\ln\gamma_i=1-\ln(1-x_jA_{j/i})-\frac{x_i}{1-x_jA_{j/i}}-\frac{x_j\left(1-A_{i/j}\right)}{1-x_iA_{i/j}} \tag{20}$$

where $A_{i/j}$ and $A_{j/i}$ are the adjustable parameters. From the Wilson equation, the activity of ternary or higher components can be investigated using only parameters obtained from binaries.

The pair of parameters $A_{i/j}$ and $A_{j/i}$ could be obtained through the values of $\ln\gamma_i^{x_i\to0}$ and $\ln\gamma_j^{x_j\to0}$ based on the binary infinitely dilute activity coefficients as follows[46]:

$$\ln\gamma_i^{x_i\to0}=-\ln\left(1-A_{j/i}\right)+A_{i/j} \tag{21}$$

$$\ln\gamma_j^{x_j\to0}=-\ln\left(1-A_{i/j}\right)+A_{j/i} \tag{22}$$

Although the values of $\ln\gamma_i^{x_i\to0}$ and $\ln\gamma_j^{x_j\to0}$ could be obtained from experimental data, the limited experimental data makes the calculation difficult. Therefore, Miedema model is proposed in the present work for theoretic calculation. In Miedema model, the heat of formation ($\Delta H_{ij}$) of binary liquid *i-j* system could be deducted as Eq.(23)[47]:

$$\Delta H_{ij}=\frac{f_{ij}x_i[1+u_ix_j(\varphi_i-\varphi_j)]x_j[1+u_jx_i(\varphi_j-\varphi_i)]}{x_i[1+u_ix_j(\varphi_i-\varphi_j)]V_i^{\frac{2}{3}}+x_j[1+u_jx_i(\varphi_j-\varphi_i)]V_j^{\frac{2}{3}}} \tag{23}$$

The $f_{ij}$ is calculated by Eq.(24) [47]:

$$f_{ij}=\frac{2pV_i^{\frac{2}{3}}V_j^{\frac{2}{3}}\left\{q/p\left[\left(n_{\mathrm{ws}}^{1/3}\right)_i-\left(n_{\mathrm{ws}}^{1/3}\right)_j\right]^2-\left(\varphi_i-\varphi_j\right)^2-b\left(r/p\right)\right\}}{\left(n_{\mathrm{ws}}^{1/3}\right)_i^{-1}+\left(n_{\mathrm{ws}}^{1/3}\right)_j^{-1}} \tag{24}$$

where $\varphi$ is the electron density, $V$ is the molar volume and $n_{\mathrm{ws}}$ is the averaged electron density at the boundary of the Wigner-Seitz cell. For all alloys $q/p$ equals 9.4 $V^2/(du)^{2/3}$. The values for $p$, used in calculating numerical of $f_{ij}$ are 14.1, 10.6 and 12.3 for alloys of two transition metals, two non-transition metals, and a transition metal with a non-transition metal, respectively. $b$ equals 1.0 for solid alloys and 0.73 for liquid alloys of a transition metal with a non-transition metal, and equals 0 for the others alloys.

The excess molar Gibbs free energy in *i-j* binary system, $\Delta G_i^{\mathrm{E}}$, could be expressed as Eq.(25):

$$\Delta G_i^{\mathrm{E}}=RT\ln\gamma_i \tag{25}$$

The relationship between $\Delta G_i^{\mathrm{E}}$ and the total excess molar Gibbs free energy, $G_{ij}^{\mathrm{E}}$, of the *i-j* binary system is given by Eq.(26)[48]:

$$\Delta G_i^{\mathrm{E}}=G_{ij}^{\mathrm{E}}+\left(1-x_i\right)\frac{\partial G_{ij}^{\mathrm{E}}}{\partial x_i} \tag{26}$$

and $G_{ij}^{\mathrm{E}}$ could be obtained by Eq.(27):

$$G_{ij}^{\mathrm{E}}=\Delta H_{ij}-TS_{ij}^{\mathrm{E}} \tag{27}$$

where $T$ is the temperature of the liquid melt (1273 K in present work), $S_{ij}^{\mathrm{E}}$ represents the excess entropy of mixing and could be approximately calculated by Eq.(28)[49]:

$$S_{ij}^{\mathrm{E}}=0.1\times\Delta H_{ij}\left(\frac{1}{T_{\mathrm{m}_i}}+\frac{1}{T_{\mathrm{m}_j}}\right) \tag{28}$$

where $T_{\mathrm{m}i}$ is the melting point of component *i*.

From Eqs.(23~28), the activity coefficient of component *i* in infinite solution *j*, $\ln\gamma_i^{x_i\to0}$, could be deduced as Eq.(29):

$$\ln\gamma_i^{x_i\to0}=\frac{\alpha_{ij}f_{ij}\left[1+u_i\left(\varphi_i-\varphi_j\right)\right]}{RTV_j^{2/3}} \tag{29}$$

where $\alpha_{ij}$ is donated as Eq.(30):

$$\alpha_{ij}=1-0.1T\left(\frac{1}{T_{\mathrm{m}i}}+\frac{1}{T_{\mathrm{m}j}}\right) \tag{30}$$

The values of same parameters used for $\gamma_i$ calculation are listed in Table 1[49]. Then the value of $\alpha_{\mathrm{Al}}$ could be obtained by Eq.(18). The calculated $a_{\mathrm{Al}}^{\mathrm{I}}$, $\alpha_{\mathrm{Al}}$ and $\Delta\mu$ are listed in Table 2. For comparison, the values of $k$ from experimental data fitting and theoretical calculation are listed in Table 3. Since the data of Al-10Mg/graphite fabrics are very scattered, they are not shown in Fig.8 and Table 3.

**Table 1 Values of parameters used for $\gamma_i$ calculation[49]**

| Element | $n_{\mathrm{ws}}$/d.u. | $\Phi$/V | $V^{2/3}$/cm$^2$ | $T_{\mathrm{m}}$/K | $u$ | $r/p$ |
|---|---|---|---|---|---|---|
| Al | 2.69 | 4.20 | 4.6 | 933 | 0.07 | 1.9 |
| Mg | 1.60 | 3.45 | 5.8 | 922 | 0.10 | 0.4 |

Note: $q/p$=9.4, $b$=0, $p$=14.1, $T$=1273 K

**Table 2 Calculation results of $a_{\mathrm{Al}}^{\mathrm{I}}$, $\alpha_{\mathrm{Al}}$ and $\Delta\mu$**

| Parameter | Al-3.2Mg | Al-4.5Mg | Al-6.5Mg | Al-8.5Mg | Al-10Mg | Al-13Mg | Al-17Mg |
|---|---|---|---|---|---|---|---|
| $a_{\mathrm{Al}}^{\mathrm{I}}$ | 0.0334 | 0.0334 | 0.0334 | 0.0334 | 0.0334 | 0.0334 | 0.0334 |
| $\alpha_{\mathrm{Al}}$ | 0.964 | 0.950 | 0.928 | 0.900 | 0.889 | 0.867 | 0.820 |
| $\Delta\mu$/kJ·mol$^{-1}$ | 35.59 | 35.43 | 35.19 | 34.86 | 34.73 | 34.46 | 33.88 |

**Table 3 Experimental data fitting and theoretical calculation results of $k$ (s$^{-1}$)**

| Alloy | Al-3.2Mg | Al-4.5Mg | Al-6.5Mg | Al-8.5Mg | Al-10Mg | Al-13Mg | Al-17Mg |
|---|---|---|---|---|---|---|---|
| Data-fitting | 0.00486 | 0.00431 | 0.00455 | 0.00440 | 0.0041 | 0.00584 | 0.00363 |
| Calculation | 0.00470 | 0.00468 | 0.00465 | 0.00460 | 0.00458 | 0.00455 | 0.00448 |

The values of $\Delta\mu$ decrease slightly with increasing of Mg amount (Table 2). Furthermore, the experimental or theoretical kinetic constant ($k$) changes little with increasing of Mg amount. Contreras et al[50] also concluded that Mg content did not affect significantly the spreading rate in Al-Mg alloy/TiC system. Moreover, it is obvious that theoretical calculation values of $k$ are very close to the experimental results, which indicates the applicability of above equations.

## 3 Conclusions

1) All wetting curves of Al-Mg/graphite fabrics consist of three kinetic stages, regardless of Mg amount.

2) The initial contact angle decreases from 115º in Al-3.2Mg/graphite fabrics to 88.5º in Al-17Mg/graphite fabrics system. The final contact angle decreases from 96.7º in Al-3.2Mg/graphite fabrics to 71º in Al-17Mg/graphite fabrics system.

3) Since microstructures of graphite fiber surface are mainly composed of graphitic basal planes, the initial contact angle measured on porous M40 graphite fabrics is lower than reported results on dense carbon plates.

4) Due to decrease of surface tension of Al-Mg alloys, the initial and final contact angles decrease with increasing the Mg amount.

5) The experimental or theoretical $k$ changes little with increasing of Mg amount. Moreover, theoretical calculation values of $k$ are very close to the experimental results, which indicate the applicability of Miedema model to the calculation of kinetic constant.

## References


1 Yang H F, Fu P F. *Surface Review and Letters*[J], 2008, 15(4): 337

2 Zhou J M, Zheng W Q, Qi L H *et al*. *Rare Metal Materials and Engineering*[J], 2015, 44(8): 1851

3 Zhang Y H, Wu G H. *Transactions of Nonferrous Metals Society of China*[J], 2010, 20(11): 2151

4 Zhang Y H, Wu G H. *Rare Metals*[J], 2010, 29(1): 102

5 Matsunaga T, Ogata K, Hatayama T *et al*. *Composites Part A*[J], 2007, 38(3): 771

6 Landry K, Kalogeropoulou S, Eustathopoulos N. *Materials Science and Engineering A*[J], 1998, 254(1-2): 99

7 Nakae H, Yamamoto K, Sato K. *Materials Transactions JIM*[J], 1991, 32(6): 531

8 Daoud A. *Materials Science and Engineering A*[J], 2005, 391(1-2): 114

9 Hufenbach W, Gude M, Czulak A *et al*. *Materials Science Forum*[J], 2011, 690(2): 116

10 Blucher J T, Narusawa U, Katsumata M *et al*. *Composites Part A*[J], 2001, 32(12): 1759

11 Matsunaga T, Matsuda K, Hatayama T *et al*. *Composites Part A*[J], 2007, 38(8): 1902

12 Zhou Y X, Xia Y M. *Composites Science and Technology*[J], 2001, 61(14): 2025

13 Seong H G, Lopez H F, Robertson D P *et al*. *Materials Science and Engineering A*[J], 2008, 487(1-2): 201

14 Wu G H, Su J, Gou H S *et al*. *Journal of Materials Science*[J], 2009, 44(18): 4776

15 Wang X, Chen G Q, Yang W S *et al*. *Materials Science and Engineering A*[J], 2011, 528(28): 8212

16 Rams J, Urena A, Escalera M D *et al*. *Composites Part A*[J], 2007, 38(2): 566

17 Urena A, Rams J, Escalera M D *et al*. *Composites Science and Technology*[J], 2005, 65(13): 2025

18 Tang Y P, Liu L, Li W W *et al*. *Applied Surface Science*[J], 2009, 255(8): 4393

19 Urena A, Rams J, Escalera M D *et al*. *Composites Part A*[J], 2007, 38(8): 1947

20 Shi J, Che R C, Liang C Y *et al. Composites Part B*[J], 2011, 42(6): 1346

21 Han D S, Jones H, Atkinson H V. *Journal of Materials Science*[J], 1993, 28(10): 2654

22 Yoshida M, Matsunaga T, Ogata K *et al*. *Materials Science Forum*[J], 2007, 877: 539

23 Wang C C, Chen G Q, Wang X *et al*. *Metallurgical and Materials Transactions A*[J], 2012, 43(7): 2514

24 Wang X, Jiang D M, Wu G H *et al*. *Materials Science and Engineering A*[J], 2007, 497(1-2): 31

25 Liu G W, Muolo M L, Valenza F *et al*. *Passerone, Ceramics International*[J], 2010, 36(4): 1177

26 Landry K, Rado C, Voitovich R *et al*. *Acta Materialia*[J], 1997, 45(7): 3079

27 Wang X, Wang C C, Chen G Q *et al*. *Surface Review and Letters*[J], 2013, 20(3-4): 3

28 Kostikov V I, Koshelev Y I, Filimonov E F *et al. Poroshkovaya Metallurgiya*[J], 1981, 20(10): 83

29 Landry K, Eustathopoulos N. *Acta Materialia*[J], 1996, 44(10): 3923

30 Rangel E R, Guerrero M. *Journal of Ceramic Processing Research*[J], 2006, 7(1): 66

31 Wang D J. Wu S T. *Acta Metallurgica et Materialia*[J], 1994, 42(12): 4029

32 Xiu Z Y, Yang W S, Chen G Q *et al*. *Materials and Design*[J], 2012, 33: 350

33 Wang S R, Wang Y Z, Wang Y *et al. Journal of Materials Science*[J], 2007, 42(18): 7812

34 Yang L L, Shen P, Lin Q L *et al*. *Materials Chemistry and Physics*[J], 2010, 124(1): 499

35 Levi G, Bamberger M, Kaplan W D. *Acta Materialia*[J], 1999, 47(14): 3927

36 Dai Z S, Shi F H, Zhang B Y *et al. Applied Surface Science*[J], 2011, 257(15): 6980

37 Donnet J B, Brendle M, Dhami T L *et al. Carbon*[J], 1986, 24(6): 757

38 Garciacordovilla C, Louis E, Pamies A. *Journal of Materials Science*[J], 1986, 21(8): 2787

39 He P, Liu Y Z, Liu D. *Materials Science and Engineering A*[J], 2006, 422(1-2): 333
40 Dezellus O, Hodaj F, Eustathopoulos N. *Journal of the European Ceramic Society*[J], 2003, 23(15): 2797
41 Landry K, Kalogeropoulou S, Eustathopoulos N. *Materials Science and Engineering A*[J], 1998, 254(1-2): 99
42 Dezellus O, Hodaj F, Eustathopoulos N. *Acta Materialia*[J], 2002, 50(19): 4741
43 Laha T, Kuchibhatla S, Seal S *et al*. *Acta Materialia*[J], 2007, 55(3): 1059
44 Lu L, Dahle A K, StJohn D H. *Scripta Materialia*[J], 2006, 54(12): 2197
45 Wilson G M. *Excess Free Energy of Mixing*[J], 1964, 86(2): 127
46 Tao D P. *Metallurgical and Materials Transactions B*[J], 2011, 32(6): 1205
47 Miedema A R, Dechatel P F, Deboer F R. *Physica B*[J], 1980, 100(1): 1
48 Revzin B, Fuks D, Pelleg J. *Composites Science and Technology*[J], 1996, 56(1): 3
49 Tanaka T, Gokcen N A. *Journal of Phase Equilibria*[J], 1995, 16(1): 10
50 Contreras A, Bedolla E, Perez R. *Acta Materialia*[J], 2004, 52(4): 985

# Al-Mg 合金在 2D-石墨纤维织物上的润湿性及铺展动力学分析

王晨充[1]，黄明浩[1]，张秋红[1]，王　旭[2]
(1. 东北大学 轧制技术及连轧自动化国家重点实验室，辽宁 沈阳 110819)
(2. 辽宁石油化工大学，辽宁 抚顺 113001)

**摘　要**：采用固位液滴法分析了不同 Mg 含量（3.2%, 4.5%, 6.5%, 8.5%, 10%, 13%, 17%，质量分数，下同）的 Al-Mg 合金在 M40 石墨纤维织物上的润湿行为。详细讨论了镁含量对合金润湿性和铺展行为的影响。在 Al-Mg/石墨织物体系中，初始接触角由 3.2%Mg 的 115°降低到 17%Mg 的 88.5°。最终接触角由 3.2%Mg 的 96.7°下降到 17%Mg 的 71°。由于 M40 多孔石墨织物的表面微观结构与碳板具有明显的区别，在 M40 多孔石墨织物上测得的初始接触角均低于在致密碳板上测得的结果。由于 Al-Mg 合金表面张力的降低，初始接触角和最终接触角随着 Mg 含量的增加而减小。根据 Dezellus 方程，对实验结果进行数据拟合，得到了铺展行为的动力学常数 *k* 值。同时，采用 Miedema 模型计算了理论 *k* 值。实验和理论结果均显示，随 Mg 含量的增加 *k* 值无显著变化。此外，*k* 的理论计算值与实验结果基本吻合，证明了 Miedema 模型对 Al-Mg/石墨织物体系中动力学常数计算的适用性。

**关键词**：复合材料；润湿；铺展；Al-Mg 合金；石墨纤维

---

作者简介：王晨充，男，1988 年生，博士，讲师，东北大学材料科学与工程学院，辽宁 沈阳 110819，电话：024-83680246，E-mail: wangchenchong@ral.neu.edu.cn